Bioconjugate Chemistry

Article

A facile approach for synthesis and intracellular delivery of size tunable cationic peptide functionalized gold nanohybrids in cancer cells

Kavita Bansal, Mohammad Aqdas, Munish Kumar, Rajni Bala, Sanpreet Singh, Javed Naim Agrewala, O. P. Katare, Rohit Kumar Sharma, and Nishima Wangoo

Bioconjugate Chem., **Just Accepted Manuscript** • DOI: 10.1021/acs.bioconjchem.7b00772 • Publication Date (Web): 28 Feb 2018

ACS Publications

Bioconjugate Chemistry is published by the American Chemical Society. 1155 Sixteenth Street N.W., Washington, DC 20036

A Facile Approach for Synthesis and Intracellular Delivery of Size Tunable Cationic Peptide Functionalized Gold Nanohybrids in Cancer Cells

Kavita Bansal[1], Mohammad Aqdas[2], Munish Kumar[3], Rajni Bala[3], Sanpreet Singh[2], Javed N. Agrewala[2], O.P. Katare[4], Rohit K. Sharma[3*] and Nishima Wangoo[5*]

[1]*Centre for Nanoscience & Nanotechnology, Panjab University, Sector-25, Chandigarh-160014, India*

[2]*CSIR-Institute of Microbial Technology, Chandigarh-160036, India*

[3]*Department of Chemistry & Centre for Advanced Studies in Chemistry, Panjab University, Sector-14, Chandigarh-160014, India*

[4]*University Institute of Pharmaceutical Sciences, Panjab University, Sector-14, Chandigarh-160014, India*

[5]*Department of Applied Sciences, University Institute of Engineering & Technology (U.I.E.T.), Panjab University, Sector-25, Chandigarh-160014, India*

*Corresponding authors:

Email: nishima@pu.ac.in (N. Wangoo), rohitksg@pu.ac.in (R.K. Sharma)

Abstract: Peptide based drug delivery system has found a mainstay in contemporary medicinal field resulting in the design and development of better pharmaceutical formulations. However, most of the available reports employ tedious multiple reaction steps for the conjugation of bioactive cationic peptides with drug delivery vehicles. To overcome these limitations, the present work describes a one-step approach for facile and time efficient synthesis of highly cationic cell penetrating peptide functionalized gold nanoparticles and their intracellular delivery. The nanoconstruct was synthesized by the reduction of gold metal ions utilizing cell penetrating peptide (CPP), which facilitated the simultaneous synthesis of metal nanoparticles and the capping of the peptide over the nanoparticle surface. The developed nanoconstruct

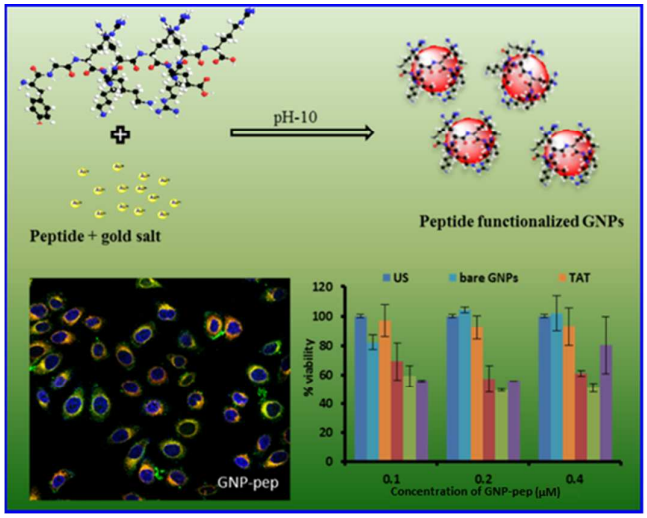

was thoroughly characterized and tested for intracellular delivery into HeLa cells. Intriguingly, a high payload of cationic peptide over gold particles was achieved, in comparison to conventional conjugation methods. Moreover, this method also provides the ability to control the size and peptide payload of nanoparticles. Produced nanoconstructs showed enhanced cancer cell penetration (μM) and significant cytotoxic effect compared to unlabeled gold nanoparticles. Therefore, this novel approach may also have significant future potential to kill intracellular hidden dreaded pathogens like human immunodeficiency virus, *Mycobacterium tuberculosis*, etc.

Introduction:

Over the last few years, medicinal chemistry has seen a tremendous rise in the used of functional peptides. Peptides are enriched with unique properties such as small size, high specificity, limited toxicity, ease of synthesis and facile surface modification. Owing to their high biocompatibility and diverse nature, peptides have gained considerable impetus and become an integral part of targeted drug delivery system. Among peptides, CPPs in particular, have gained a lot of attention in the recent years. CPP are peptides used to increase the cellular internalization of high molecular weight molecules for instance DNA, proteins and fat insoluble drugs[1]. It has been reported that the transcriptional activator of transcription (TAT) protein of Human Immunodeficiency Virus-1 (HIV-1) could be efficiently internalized into cells when present in the surrounding tissue culture media[2-4]. The domain which is responsible for this translocation is a short basic region comprised of 47-57 residues (YGRKKRRQRRR) bearing six arginine and two lysine molecules. These positively charged residues facilitate the cellular uptake by initial interactions of the peptide with negatively charged residues of heparin sulfate proteoglycans[5-7]. TAT is the most frequently used CPP for functionalization of nanoparticles to increase their overall efficiency and specificity as delivery system[8, 9]. Among various nanoparticles, gold nanoparticles (GNPs) are of significant

interest as delivery vehicle due to their considerable proven bio-compatibility and unique optical properties[10] induced by surface plasmon resonance (SPR) of GNPs surface[11]. Moreover, the ability to functionalize the GNPs by multiple ligands (chemical and biomolecules) with high loading capacity makes them an excellent candidate for applications such as in drug delivery, labeling, sensing and imaging[12-14].

For the conjugation of peptides with nanomaterials different approaches are being reported, for instance, electrostatic interaction between peptide and nanoparticles having opposite charge, use of thiol or biotin motif peptides for direct conjugation with gold and stratavidin modified gold nanoparticles respectively[15-17]. However, these conjugation techniques suffer from various shortcomings such as weak peptide-nanoparticle interaction and prerequisite of specific molecules. Moreover, highly stable covalent attachment among peptide and GNPs requires the use of various coupling reagents and involves tedious multi-step reactions. Earlier report by Fuente *et al.*[18] encompassed the introduction of TAT peptide onto GNPs via the carbodiimide coupling reaction. The process involved the formation of tiotropin capped GNPs in methanol/acetic acid media using sodium borohydride as reducing agent. Here, tiopronin was used to generate the carboxylic functionalities over GNPs surface, so that EDC/NHS activated carboxyl groups can form an amide bond with the amine moiety of the peptide. Moreover, the phase transfer methodology has also been reported for the synthesis of cationic/ anionic peptides functionalization GNPs using ligand exchange process by employing 11-amino-1-undecanethiol[19]. However, this approach also comprises the multiple step reaction process. In contrast to the earlier mentioned peptide-nanoparticle binding methodologies, Slocik *et al.* synthesized GNP-peptide complex by reducing the gold salt directly with dodecyl A_3 peptide (AYSSGAPPMPPF)[20] . In another reports, the Rev and RGD peptides retain their anticancer and $\alpha_v\beta_3$ integrin targeting efficiency respectively even after reducing the gold salt[21-23]. Additionally, the antimicrobial peptide conjugated GNPs

synthesized by one step methodology showed high antimicrobial activity and serum stability compared to alone peptide[24]. Indeed, bonding between peptide and GNPs primarily depends upon the amino acid sequence and studies reveal that it is comparatively difficult to conjugate the cationic peptides with metallic nanoparticles than anionic peptide[25]. Peptides having terminal cationic residue (cysteine, arginine, serine and tryptophan) may lead to aggregation of negatively charged GNPs in aqueous solution[26]. DLVO theory implies that the strong attractive Vander waals forces between charged nanoparticles are responsible for their aggregation, which can be balanced by generating electrostatic repulsive forces in the colloidal solution by introduction of opposite charged molecules[27]. Ojea-jimenez *et al.* confirmed this theory by evaluating the effect of various charged molecules on the stability of citrate capped GNPs. Results confers that the negatively charged molecules ending with R-COO^- retains the stability of solution by overcoming the Vander waals attraction, whereas species ended with R-$COOH^-$ or R-NH_3^+ terminals increase the attractive interaction forces and resulting the aggregation of nanoparticles[28]. Hence, a lot of optimizations and multiple chemical reagents are prerequisite to acquire a stable cationic peptide capped GNPs complex in aqueous media.

Keeping in view the above mentioned points, we propose a facile, eco-friendly, one-step approach for bio-conjugation of highly cationic TAT peptide with GNPs in aqueous medium. In this method, peptide serves the dual role of reducing as well as stabilizing agent to synthesize the peptide capped gold nanohybrids. The synthesized conjugates showed excellent stability in aqueous medium even at room temperature without any further addition of stabilizing agent. Also, *In-vitro* results showed enhanced cell penetration and anti-proliferation effect of TAT-GNPs hybrids in HeLa cells compared to GNPs alone, thereby proving their significant potential in drug delivery applications.

Results and Discussion

Synthesis of size tuned GNPs at basic pH:

The GNPs were synthesized using chemical methodology employing TAT peptide as reducing as well as capping agent. The effect of pH and peptide concentration on the formation of nanoparticles was carefully studied. For this, 20 µl of different concentration of peptide was used for the synthesis of GNPs at varying pH (9, 10 or 11). It was observed that the reactions carried at pH-10 having final peptide concentration of 0.16 µM ($GP_{0.16}$), 0.8 µM ($GP_{0.8}$), 1.6 µM ($GP_{1.6}$) or 3.2 µM ($GP_{3.2}$) displayed dark red colored solutions, while at 0.08 µM ($GP_{0.08}$) and 6.4µM ($GP_{6.4}$) peptide concentrations, violet and light pink color solutions were obtained respectively. However, pink or violet colored final colloidal solutions were obtained at pH 9 and 11 [fig.1 (a-c)]. It has been reported that the reduction of gold salt significantly dependent on the pH of the working solution. In the reaction process, phenolic groups present in side chain of tyrosine (TAT peptide) plays an substantial role in reduction of the Au(III) ions. Tyrosine shows enhanced reductive capability in aqueous solution at pH near the pKa value of tyrosine (~10), where all phenolic moieties are get oxidized into phenoxide[29]. Whereas, at pH 9 partial oxidation of phenolic groups leads to incomplete reduction of gold salt[30]. Moreover, at high pH (~11) low yield of GNPs can be due to the conversion of highly reactive gold ion $[AuCl_3(OH)]^-$ to less reactive state $[AuCl_2(OH)_2]^-$ and $[AuCl(OH)_3]^-$[31].

In UV-visible spectroscopy, the absorption maxima of the synthesized colloidal solutions were centered around 515 nm to 530 nm SPR band of GNPs[32] which is a clear indicative of the synthesis of stable GNPs [Fig.2 (d-f)]. Furthermore, it was evident from the TEM images that the synthesized nanoconstructs ($GP_{0.08}$, $GP_{1.6}$, $GP_{3.2}$ at pH-10) were well dispersed, nearly spherical in shape and had a core particle size of about 30 nm, 15 nm and 10 nm respectively [Fig. 1 (g-i)]. In addition, DLS analysis also confirms the high mono-dispersity (PDI<0.5) of

these nanoconstructs with hydrodynamic size of 42nm, 30.8nm and 18.2nm respectively. Size analysis data revels that with increase in peptide concentration the size of synthesized nanoconstructs decreased, which confirms the role of peptide acts as reducing agent.

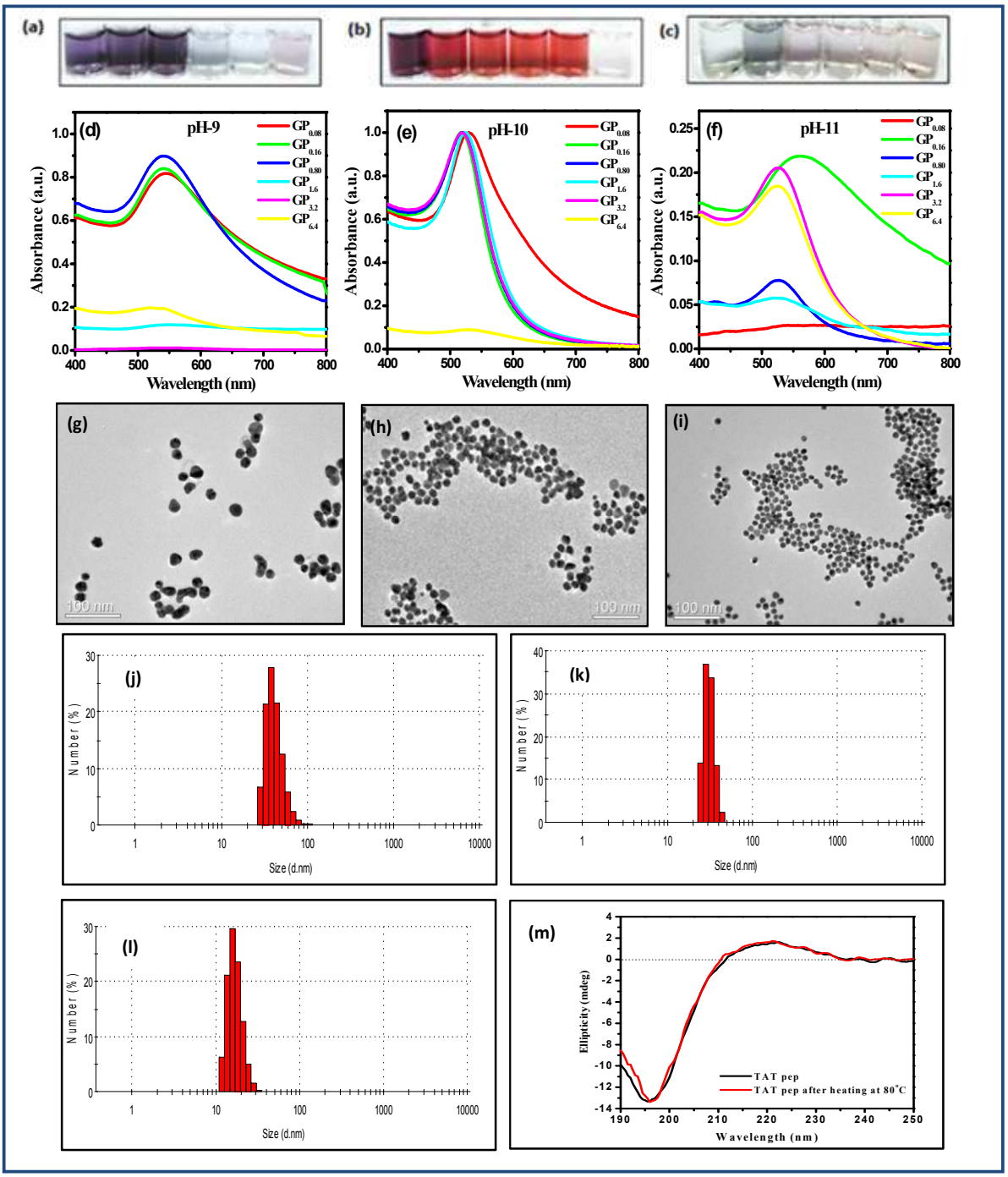

Fig. 1. Effect of pH and peptide concentration on morphology and kinetics of peptide syntheized gold nanoparticles. Color (a-c) and absorbance spectrum (d-f) of gold nanoparticles synthesized at pH 9,10 and 11 respectively**.** TEM images (g-i) of $GP_{0.08}$, $GP_{1.6}$,

$GP_{3.2}$ (at pH-10), synthesized nanoparticles are nearly spherical in shape and having mean particle size of about 30nm, 15 nm and 10 nm respectively at magnification 40000 X. Particle size distribution (j-l) of $GP_{0.08}$, $GP_{1.6}$, $GP_{3.2}$ nanoparticles obtained from DLS analysis (42nm, 30.8nm and 18.2nm respectively). Mean hydrodynamic sizes of the conjugates are usually larger than actual size of particles. Circular Dichroism spectra (m) of TAT peptide (64μM) without heating (black) and after heated at 80˚C for 1 hr. in water (red).

In order to evaluate the reaction kinetics of GNP-pep complex, various aliquots were taken at different time intervals. The reaction in aliquots was ceased by inserting the vessel in ice cold water. Absorbance of collected aliquots was monitored at 520 λ_{max} ($GP_{1.6}$) and it was observed that reduction of gold salt was almost saturated after 60 minutes [Fig. 2 (a, b)]. Furthermore, the rate for synthesis of GNP-pep complex decreased with increase in peptide concentration, which eventually delayed the nucleation and growth process of GNPs. Consequently, the above studies inferred that a small change in pH and peptide concentration during synthesis process imparts a significant effect over the structural morphology and reaction kinetics of synthesized nanoconstructs.

The CD spectrum of TAT peptide displays a strong negative band at 196 nm (-13.31 $M^{-1}cm^{-1}$) and a positive band at 222 nm (+1.62 $M^{-1}cm^{-1}$), representing the left-handed 3_1-helix conformation[33, 34] [Fig.1 (m)]. Additionally, to evaluate the effect of heating on the conformation of peptide, the peptide was heated in aqueous solution at 80˚C for 60 min., followed by cooling at room temperature (replicating conditions used in the synthesis of the nanoconstructs). The results illustrate that the peptide retains its conformation with minimal change in its ellipticity values. Hamley *et al.*[35] also confirmed (using CD spectra and SAXS) that palmitoyl-KKFFVLK amphiphile peptide self-assemblies regain their structural conformation after heating at 55 ˚C followed by cooling. Consequently, this study proves that the reported method employs a safe and facile approach for the synthesis of peptide gold nanoconstructs.

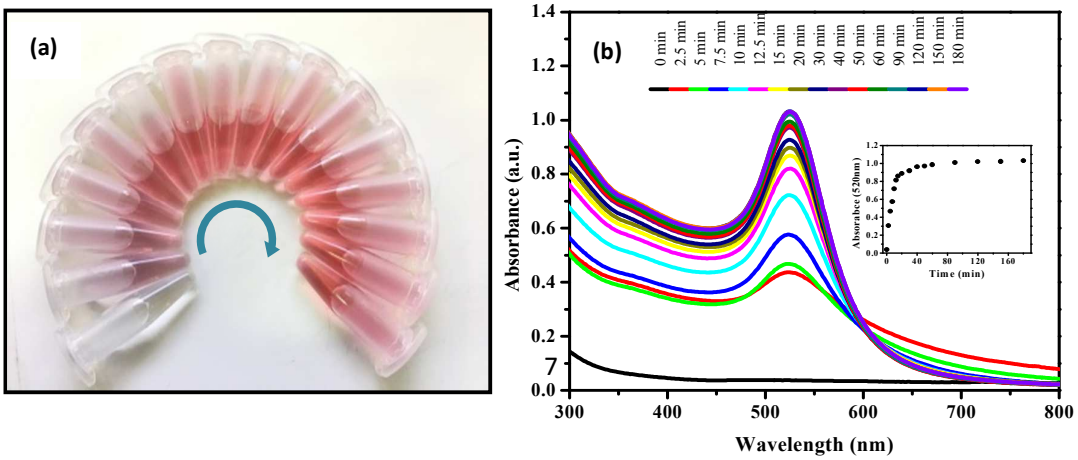

Fig. 2. Image (a) and absorption spectra (b) of various aliquots of proceeding pep-GNP complex reaction mixture, Inset shows the time-dependence absorbance of aliquots at 520 nm. The data are the representative of three independent experiments.

TAT functionalized gold nanoconstructs bearing negative charge:

In order to confirm the appropriate layering of the peptides over synthesized nanoparticles, TGA, FT-IR and ζ-potential studies were carried out. TGA was performed on the lyophilized sample of pep-GNP, GNP and pure peptide, the thermogram of pep-GNP conjugate [Fig.2a(a1)] shows a first weight loss upto 100ºC due to the evaporation of residual and physisorbed water that can be neglected. Subsequent results show a primary mass loss of 17.13% (I) between 140 to 200 °C followed by a second mass loss peak of 5.45% (II) at higher temperatures 300-350 °C. The first primary loss corresponding the capping of carbonate ions from the potassium carbonate, showing similar weight percent loss (17%) and temperature range compare to gold salt is reduced only in the presence of K_2CO_3 [Fig.2a (a2)]. Secondary loss is due to the capped peptide molecules over the gold surface, also supported by the DSC data [Fig.S2]. Whole pure peptide gets degraded in the temperature range of 200-250°C [Fig.2a (a3)], which is shifted to250-300 °C for pep-GNP, confirms that the peptide is strongly bound with the gold surface[36, 37].

In FT-IR spectra [Fig. 2a (i, ii)] the characteristic IR absorption peaks of peptides at 1642 cm^{-1} (amide I, carbonyl stretch vibration), 1625 (C=C stretch), 1543 cm^{-1} (amide II) and 1389 cm^{-1} (amide III, C–N stretch vibration) were found to be present in the corresponding spectra of pep-GNPs, signifying the capping of peptide molecules on the nanoparticles surface. Intense broad bands in the region between 3300 and 3400 cm^{-1} were representative of N-H and O-H stretching vibrations. The primary aliphatic amine peaks at 1183 cm^{-1} and 1126 cm^{-1} completely disappeared in peptide-GNPs spectra, depicts the reduction of gold salt by phenolic group of Tyrosine and free electrons of the amine group respectively[29, 38-40].

The high zeta potential values [Fig. 2 b] of the pep-GNPs complexes indicated the higher stability and therefore, their robustness as efficient candidates for drug delivery.

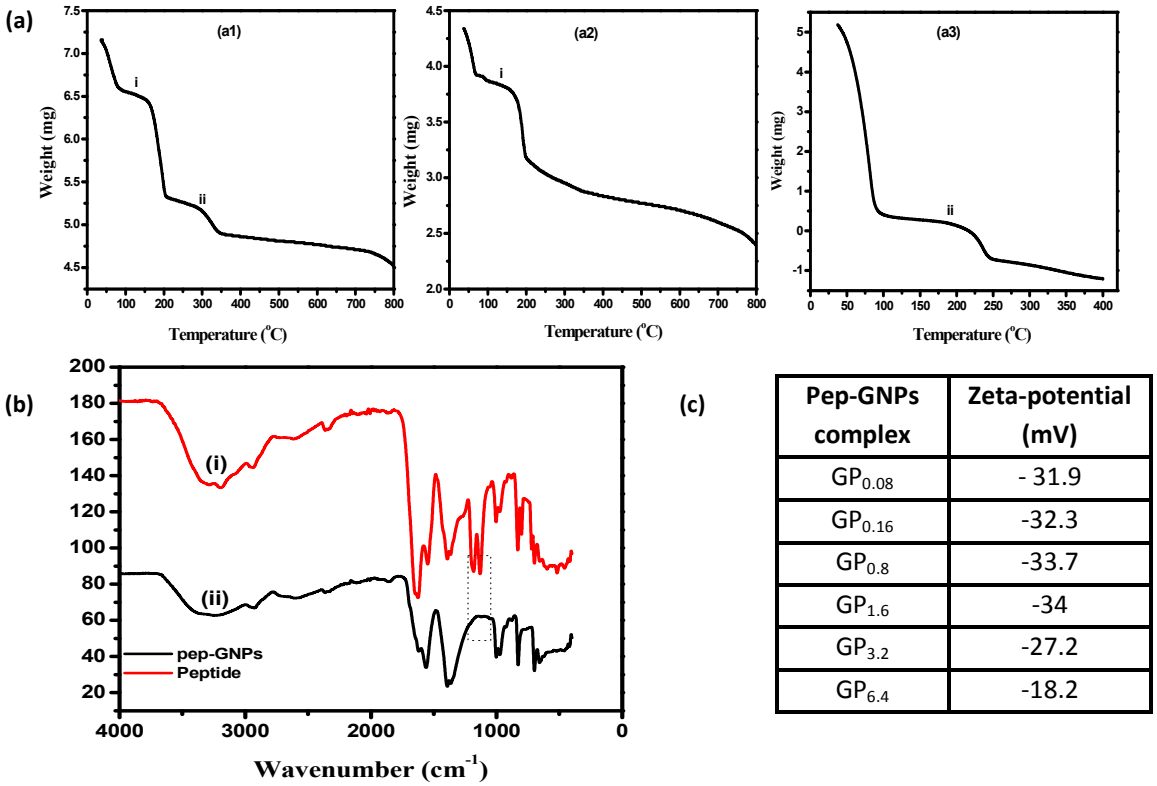

(c)

Pep-GNPs complex	Zeta-potential (mV)
$GP_{0.08}$	- 31.9
$GP_{0.16}$	-32.3
$GP_{0.8}$	-33.7
$GP_{1.6}$	-34
$GP_{3.2}$	-27.2
$GP_{6.4}$	-18.2

Fig. 2 Negatively charged GNP-peptide constructs capped with TAT peptide (a) TGA spectra of (a1) pep-GNPs, (a2) GNPs, (a3) pure peptide. (b) FT-IR spectra of (i) pure peptide (ii) pep-GNPs, (c) Zeta potential of pep-GNPs synthesized at pH 10.

In the present work, reduction of gold salt occurs and electron rich phenolic residues of tyrosine[30] and amine groups of peptide to yield the corresponding nanoconstructs in the presence of potassium carbonate [Fig. 3]. Besides, carboxylic moieties of the peptide render the synthesized GNPs stable. Further, physical adsorption of the excess peptide and carbonate ions in the solution keeps the nano particles well dispersed. In the absence of peptide, only potassium carbonate is not able to synthesize the stable GNPs [SI- Fig.2 (i)] However, the GNPs synthesized by peptide showed no aggregation even after three months [SI- Fig.2 (ii)].

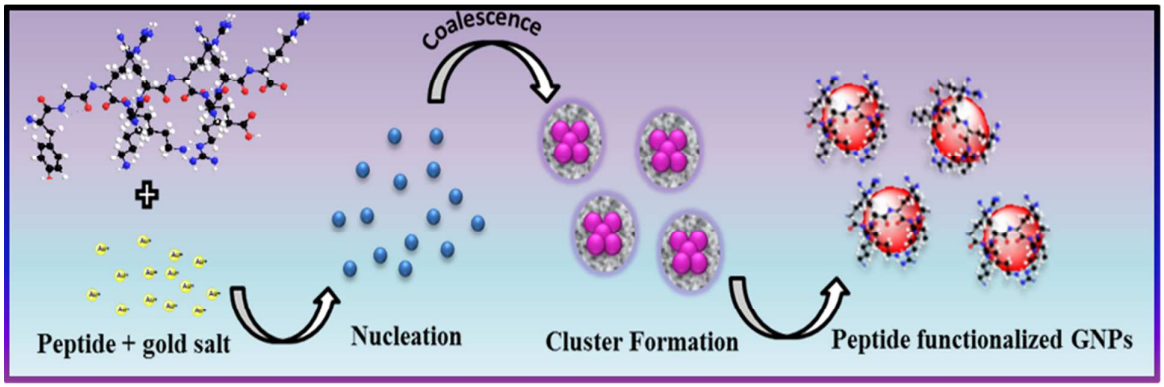

Fig. 3 Schematic representation of peptide functionalized gold nanoparticles synthesis GNPs synthesis follows two-step reaction mechanism, firstly reduction of ionic gold (Au^{3+}) into metallic gold nuclei (Au^0), subsequently the growth of nuclei in to bigger particles by coalescence[41]

High and regulated payload of peptide on peptide-GNP constructs:

Owing to the presence of arginine in the TAT peptide, Bradford assay was employed to calculate the amount of peptide capped on the GNPs surface. Arginine produces blue color on reacting with Bradford reagent, which provides a characteristic absorption band at 590 nm. Firstly, a calibration curve [Fig. 4(a)] of TAT was obtained by plotting the absorbance ratio at 590 nm and 450 nm (A_{590}/A_{450})[42, 43] followed by calculation of unreacted amount of peptide remaining in the supernatant of reaction mixture [Table 1]. Interestingly, graph [Fig. 4(b)] reveals the amount of peptide capped to nanoparticles gives a linear regression with the concentration of the peptide added during the nanoparticle synthesis. Thereby, it is possible to control the loading amount of peptide over GNPs.

Additionally, the number of peptide molecules capped over a single GNP was also calculated by considering the core size of nanoparticle obtained by TEM analysis. The average number of gold atoms (N) in one gold nanoparticle were calculated by Eq.1 assuming that all the synthesized particles are spherical in shape and have uniform fcc structure, here ρ is the density for fcc gold (19.3 g/cm^3) and M stands for atomic weight of gold (197 g/mol). Total number of gold nanoparticles (N_t) and the molar concentration (C) of the nanoparticles in

solution was calculated using Eq. 2,3, here W is weight of gold solution taken (Mol. wt.$HAuCl_4.3H_2O$=393.83), N_A is the Avogadro's constant and V is the volume of the reaction solution[44, 45]. Remarkably, a high payload of TAT peptide i.e. 144, 427 and 24 molecules was found to be conjugated on one nanoparticle of the synthesized $GP_{0.08}$, $GP_{1.6}$ and $GP_{3.2}$ nanoconstructs respectively. TGA studies also confirmed the high loading of peptide molecules over the gold nanoconstruct (SI). Sanz *et al*. reported that the addition of more than 1 µg/ml (0.7 µM) of TAT peptide leads to aggregation of GNPs during covalent coupling process and number of TAT chains bound to GNPs is directly proportional to the initial concentration of peptide in reaction mixture[46]. Hence, our proposed methodology gives the benefits of functionalization the GNPs with approximately 4.5 times higher payload of TAT peptide ($GP_{3.2}$) in a facile manner. Furthermore, approximately 83% of added peptide was utilized in reduction and capping of GNPs, which reflects its high utility to be used as novel procedure for synthesis of cationic peptide functionalized gold conjugates.

$$N = \frac{\pi \rho D^3}{6M} = 30.89602D^3 \quad \text{..... (Eq.1)}$$

$$N_t = \frac{W \times N_A}{393.83 \times N} \quad \text{..... (Eq.2)}$$

$$C = \frac{N_t}{V \times N_A} = \frac{W\,(gm)}{393.83 \times V(l) \times N} \quad \text{..... (Eq.3)}$$

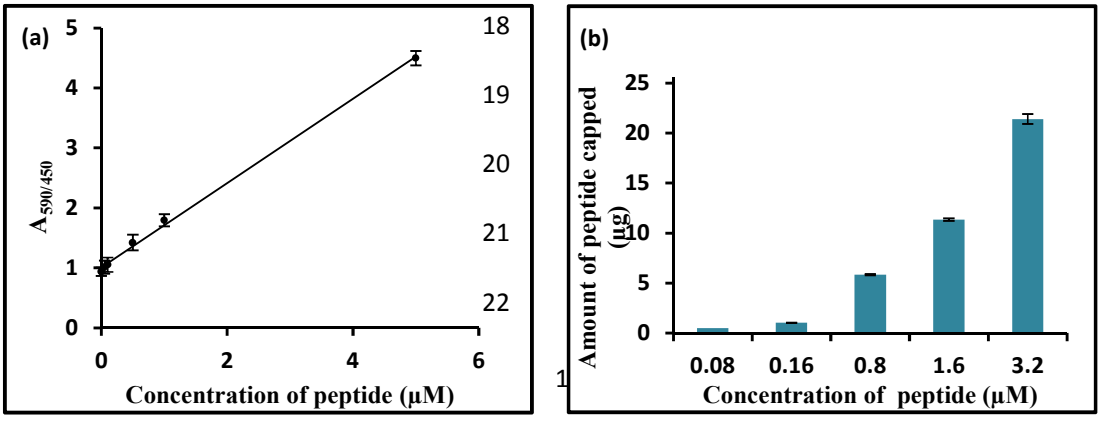

Fig. 4 Quantification of the amount of peptide capped on GNPs. (a) Standard calibration plot and the amount of peptide capped to nanoparticles (b) of TAT peptide.

Table 1 Calculated amount of peptide capped over GNPs

	Quantity of peptide added (µg)	Quantity of peptide in supernatant (µg)	Quantity of peptide capped on gold particles (µg)
$GP_{0.08}$	0.624	0.140	0.484
$GP_{0.16}$	1.284	0.266	1.017
$GP_{0.8}$	6.240	0.399	5.841
$GP_{1.6}$	12.480	1.138	11.342
$GP_{3.2}$	24.960	3.572	21.388

High colloidal stability of GNP-peptide constructs at physiological conditions:

Colloidal GNPs are highly susceptible to aggregation in the presence of electrolytes. Therefore, it is essential to examine the stability of synthesized nanohybrids in physiological ionic conditions, in order for them to be used as potential drug carriers[47]. For this, the stability of different pep-GNP complexes were examined in phosphate buffer saline solutions and the change in SPR band at 520 nm was detected, which is a characteristic feature of GNPs stability. As the stability of GNPs decreases, it leads to agglomeration and the absorption maximum is shifted to higher wavelength. The percentage change in absorbance intensity of GNPs-peptide complexes [Fig. 5] was calculated at increasing concentrations of PBS (1X=150 mM of NaCl and 10 mM of phosphate). All the studied conjugates showed high stability in 1X PBS solution which corresponds to the tonicity of physiological fluids. As expected, $GP_{1.6}$ exhibited maximum stability in PBS solutions owing to high loading of peptide molecules over their surface. Consequently, all the synthesized pep-GNPs conjugates of different sizes are applicable for biological based systems.

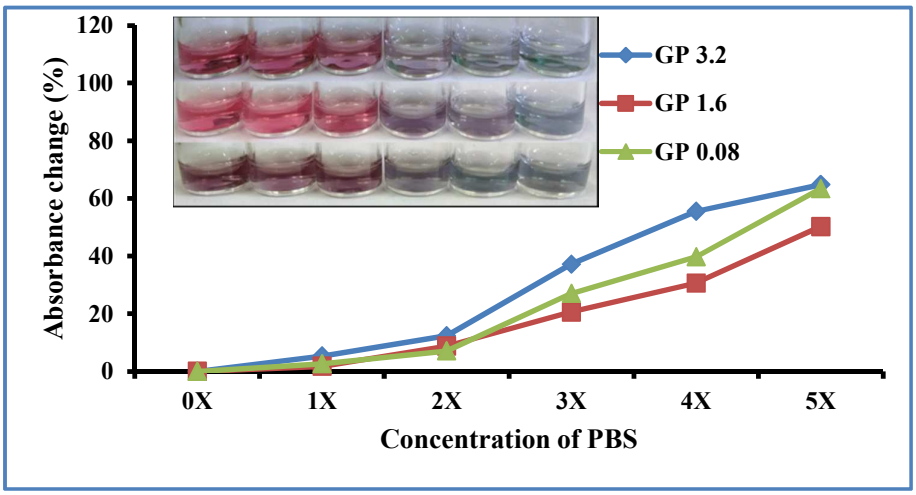

Fig. 5 Stability studies of conjugates in phosphate buffer saline (PBS). Percentage change in intensity of GNP-pep1, GNP-pep3 and GNP-pep5 at different concentrations of phosphate buffer saline solution (0-5X)

Anti-proliferation and enhanced cellular uptake of GNP-peptide complex:

MTT results showed that the viability percentage of Hela cells decreased significantly ($p<0.05$ and $p<0.001$) from 70% to 50% (0.2μM) after treating with GNP-Pep conjugates for 6h and 24h respectively, which illustrate that the survival of cells is time dependent [Fig. 6 (a, b)]. While, cells treated with the bare GNPs and alone TAT peptide exhibit high survival rate. Additionally, the results suggest that the $GP_{1.6}$ conjugate showed the maximum damage to the cell, which can be explained by its highest loading of peptide over their surface amongst the studied conjugates.

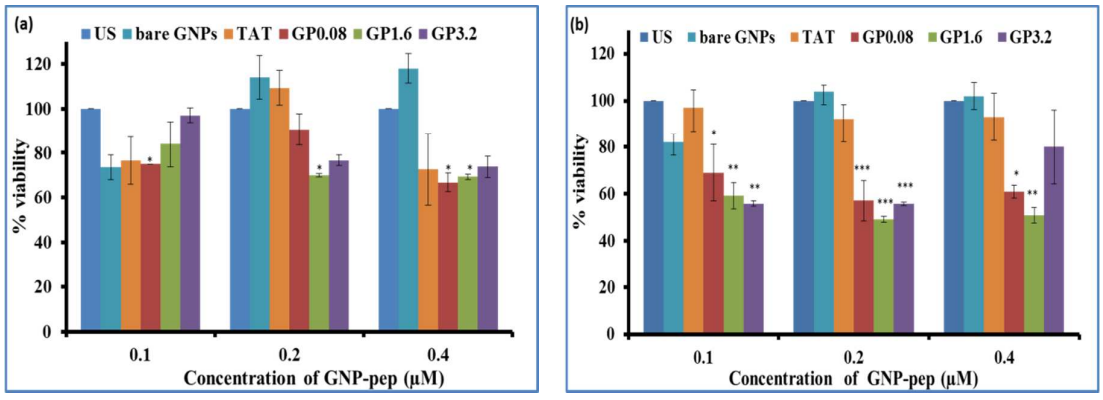

Fig.6 Cell viability studies for GNP-pep nanoconstructs by MTT assay. Dose and time dependent cytotoxicity of bare GNPs, TAT and peptide capped GNPs (GP0.08, GP1.6, GP3.2) on the HeLa cells at different time interval of 6 h (a) and 24 h (b)

Furthermore, to visualize the cellular internalization of bare and $GP_{1.6}$ conjugate, tagging with FITC was done[48]. As shown in Fig.7, the uptake of bare GNPs in HeLa cells was negligible compared to peptide capped gold nanoconstructs. These images reveal that the TAT peptide functionalized over the GNPs surface in $GP_{1.6}$ conjugate is actually responsible for its increased cellular uptake. Moreover, Confocal Z-stack images clearly indicate that the GNP-pep was efficiently internalized with in the cell (Fig. S4). Hence, in-vitro results clearly indicate that the TAT does not lose its penetrating efficiency during the synthesis process[49, 50]. Therefore, in nutshell, peptide and GNPs hybrids synthesized by the reported facile approach are highly efficient to be used as carrier vehicles for delivery of anti-cancer drug and other biological molecules with in the cells.

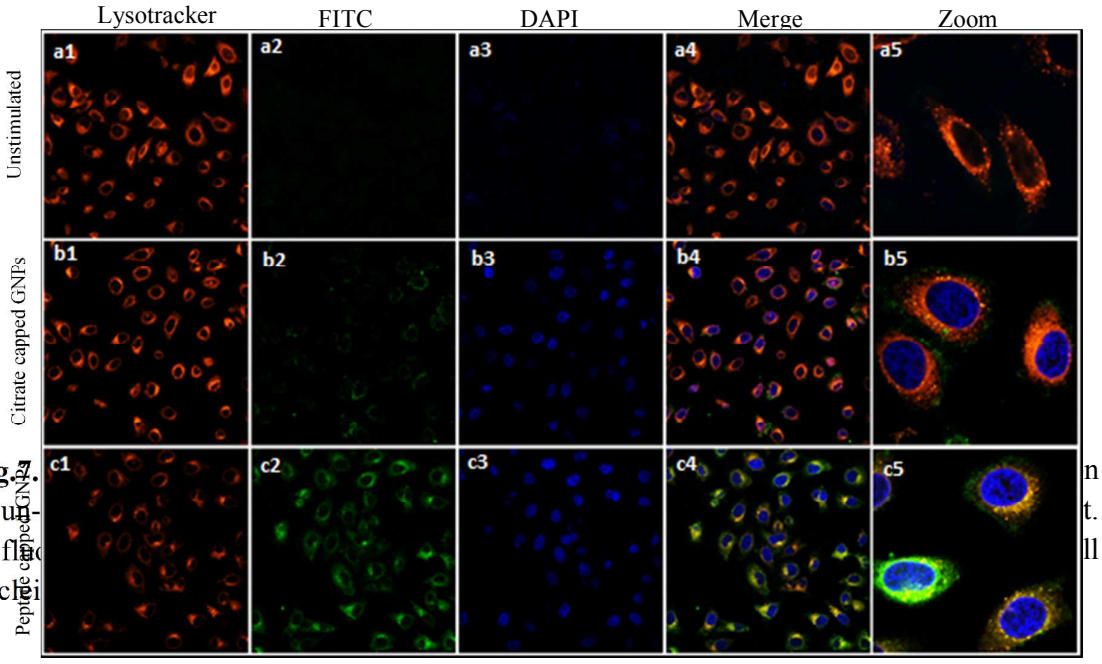

Fig.7. n
of un- t.
In fl ll
nuclei

Conclusion:

We hereby report a one pot and single step process for the functionalization of GNPs by a cell penetrating peptide (TAT) and show its intracellular internalization. In the conventional

approaches, the citrate reduced negatively charged GNPs aggregate in the presence of highly cationic TAT peptide. To overcome this problem, we have synthesized the GNP-TAT complex by direct reduction of gold salt with the TAT peptide, which subsequently capped over the gold particle surface and was confirmed by FT-IR. To optimize the reaction conditions, the synthesis was carried out at different pH and peptide concentrations. The optimum results were obtained at pH 10 and size tunable gold-peptide constructs were obtained at different peptide concentrations. The functionalization procedure is highly efficient as approximately 83% of added peptide was utilized in reduction and functionalization of GNPs. A high loading of peptide on GNPS was achieved and the calculated number of TAT peptide molecules conjugated over one nanoparticle of $GP_{0.08}$, $GP_{1.6}$ and GP nanoconstructs are 144, 427 and 24 respectively. Zeta potential and stability studies confirmed their high suitability for biological studies. The viability of cervical cancer cells (HeLa) in MTT assay was significantly reduced after treating with the $GP_{0.08}$, $GP_{1.6}$ and $GP_{3.2}$ nanoconstructs compared to bare GNPs. The cellular uptake and cell viability assay results confirmed that the TAT peptide retains its cell penetrating efficiency even after reducing the gold salt. This clearly confirms that, the peptide here serves the role of reducing agent, capping agent as well as cell penetrating agent. Hence, our method gives a new approach to functionalize highly cationic peptides with GNPs in a facile and time efficient manner. Moreover, the synthesized conjugates hold good potential to be used as a carrier vehicle in the drug delivery, biosensor and bio imaging systems.

Experimental details

Materials and methods:

Hydrogen tetrachloroaurate (III) trihydrate ($HAuCl_4.3H_2O$), trisodium citrate dehydrate (TSC), Fmoc-Arg(Pbf)-OH, Fmoc-Lys(Boc)-OH, dimethylformamide, N,N,N',N'-

Tetramethyl-O-(benzotriazol-1-yl)uroniumtetrafluoroborate (TBTU), N,N diisopropylethylamine (DIEA), piperidine, trifluoroacetic acid, diethyl ether triisopropylsilane, acetonitrile, 3-(4,5-Dimethylthiazol-2-yl)-2,5-Diphenyltetrazolium Bromide (MTT), 4,6-diamidino-2-phenylindole dihydrochloride (DAPI), Sodium dodecyl sulfate (SDS), Fluorescein isothiocyanate (FITC), Paraformaldehyde (PFA) Bradford reagent and potassium carbonate (K_2CO_3) were acquired from Sigma Aldrich (India). All the reagents used were of analytical grade and used without further purifications. All the experiments were carried out using Milli-Q water having a resistivity of 18 MΩ cm. The glassware was rinsed with aqua regia prior to use.

Synthesis of TAT peptide (YGRKKRRQRRR):

The peptide was synthesized using the standard fluorenylmethyloxycarbonyl (Fmoc) solid-phase peptide synthesis based strategy. Initially, Wang resin was employed followed by subsequent coupling steps using Fmoc-Arg(pbf)-OH, Fmoc-Gln(Trt)-OH, Fmoc-Lys(Boc)-OH, Fmoc-Gly-OH, Fmoc-Tyr(t-but)-OH,TBTU and DIEA. The intermediate Fmocdeprotection steps were carried out using 20% piperidine. The final deprotection step was performed using standard protocol (95% trifluoroacetic acid/2.5% triisopropylsilane/2.5% ELGA water) for 6h at room temperature. The crude peptide was analyzed by reverse phase high performance liquid chromatography (RP-HPLC) on a C18 column and then characterized by matrix assisted laser desorption-ionization/time-of-flight (MALDI-TOF) mass spectrometry [Fig.S1].

Synthesis of peptide reduced/functionalized gold nanoparticles (pep-GNPs):

Briefly, an aqueous solution of 0.4 mM $HAuCl_4$ (5 mL) was heated at 80˚C followed by the addition of 20 µl of peptide solution (varying concentration) and pH was adjusted using 0.5

M K_2CO_3. Initially, the color of the solution changed from light yellow to pink and finally to red, indicating the formation of GNPs. The reaction was further continued for 60 minutes in order to complete the synthesis of nanoparticles and allowed to cool at room temperature. The synthesized colloids were centrifuged (10,000 rpm for 15 minutes) and washed with DI water. The supernatant and pellet were collected separately and stored at 4˚C for analysis. The optimal reaction conditions were found by varying the pH and concentration ratio of gold ions/ peptide. As a reference, citrate capped GNPs were also synthesized by following the Turkevich method [41][SI].

Characterization techniques:

The UV–visible absorbance spectra of the nanoparticles were recorded using a JascoV-530 UV Vis spectrophotometer using 1 cm path length quartz cuvettes with 0.1 nm resolution. Particle size distribution and Zeta potential were analyzed using Malvern Zetasizer. FT-IR spectra of lyophilized powder of pep-GNPs complex and of pure peptide were measured. on Thermo Scientific Nicolet iS50 FT-IR spectrophotometer in the range from 500 cm^{-1} to 4500 cm^{-1}. Thermogravimetric analysis (TGA) was performed on the lyophilized samples using PerkinElmer TGA instrument. Transmission electron microscopy (TEM) studies were carried out using Hitachi (Model H-7500) transmission electron microscope operating at an accelerating voltage of 100 kV. Samples for TEM studies were prepared by placing a drop of the nanoparticles on carbon-coated TEM grids and allowed to dry for 5 min at room temperature before analysis. For cyclic dichroism (CD) analysis purified proteins were dialysed into distilled water and secondary structure analysis were performed using JASCO J-815 CD spectrometer at 64 μm concentration in 1mm path-length quartz cuvette. CD data were recorded at 20 °C in far UV range 190-250 nm at data pitch 0.5 nm, scanning speed 50 nm/min and bandwidth 1 nm.

Cell viability assay:

The HeLa cells were seeded into 96-well plates at $1x10^4$ cells/well, and incubated overnight at 37°C in a humidification incubator with 5% CO_2. Later, the cells were treated with different concentrations (0.1, 0.2, 0.4 μM) of $GP_{0.08}$, $GP_{1.6}$, $GP_{3.2}$, bare GNPs (TSC reduced) and TAT peptide, followed by incubation for 6h and 24h. Subsequently, the cells were incubated for 3-4h with MTT solution followed by the stop solution (50% dimethyl formamide + 20% SDS in water). The absorbance of the purple colored product was measured at 572 nm. Percentage viability of cells was calculated according to the following equation.

$$\%\ cell\ viability = \frac{Abs_{572}\ (treated)}{Abs_{572}(control)} \times 100$$

Cellular uptake studies:

For evaluating the cellular internalization of bare and peptide fictionalized GNPs were firstly tagged with fluorophore FITC (SI). For this, HeLa cells ($1x10^5$/ml) were plated overnight on coverslips, FITC labeled pep-GNPs and bare GNPs conjugates (200μl of 0.4 μM) were added into each well and incubated at 37°C for 6h. The cells were then treated with 300 nM Lysotraker Red (Invitrogen, Carlsbad, CA) for 30 mins to stain the acidic organelles. After staining, the cells were washed twice with 1XPBS followed by fixing with 4% PFA for 10 mins. The cells were washed thrice with PBS and the coverslip was mounted on the slide using mounting reagent (Slow fade with DAPI, Invitrogen, Carlsbad, CA). The coverslips were sealed and observed under the Nikon A1 confocal microscope (Nikon, Tokyo, Japan) using 488 nm (FITC-tagged gold particle) and 561 nm. The extent of nanoparticles internalization was observed by analyzing FITC signal in the cells.

Statistical analysis:

Statistical testing was performed by one way ANOVA for group analysis using GraphPad Prism (GraphPad Software, San Diego, CA). Differences were considered significant at a level of $p < 0.05$.

Acknowledgements: Authors thank financial support from UGC-BSR, India. KB and MA thank Panjab University, Chandigarh and INSPIRE Program, Department of Science and Technology (DST) respectively, for research fellowships. We are also grateful to Mr. Deepak Bhatt for confocal imaging and Mr. Randeep Sharma for TEM facility at CSIR-Institute of Microbial Technology, Chandigarh, India.

Supporting information available at DOI: Synthesis of TSC reduced GNPs, Tagging with fluorophore, TGA-DSC spectra and Confocal Z-stack cellular uptake images of pep-GNPs, MALDI-TOF spectrum of TAT peptide.

Conflict of interest: Authors declare no conflict of interest.

ORCID ID: Dr. Nishima Wangoo: 0000-0001-8691-1072

References

(1) Delehanty, J. B., Boeneman, K., Bradburne, C. E., Robertson, K., Bongard, J. E., and Medintz, I. L. (2010) Peptides for specific intracellular delivery and targeting of nanoparticles: implications for developing nanoparticle-mediated drug delivery. *Therapeutic delivery 1*, 411-433.

(2) Green, M., and Loewenstein, P. M. (1988) Autonomous functional domains of chemically synthesized human immunodeficiency virus tat trans-activator protein. *Cell 55*, 1179-1188.

(3) Frankel, A. D., and Pabo, C. O. (1988) Cellular uptake of the tat protein from human immunodeficiency virus. *Cell 55*, 1189-1193.

(4) Vives, E., Brodin, P., and Lebleu, B. (1997) A truncated HIV-1 Tat protein basic domain rapidly translocates through the plasma membrane and accumulates in the cell nucleus. *The Journal of biological chemistry 272*, 16010-16017.

(5) Vives, E., Richard, J. P., Rispal, C., and Lebleu, B. (2003) TAT peptide internalization: seeking the mechanism of entry. *Current protein & peptide science 4*, 125-132.

(6) Becker-Hapak, M., McAllister, S. S., and Dowdy, S. F. (2001) TAT-mediated protein transduction into mammalian cells. *Methods (San Diego, Calif.) 24*, 247-256.

(7) Tyagi, M., Rusnati, M., Presta, M., and Giacca, M. (2001) Internalization of HIV-1 tat requires cell surface heparan sulfate proteoglycans. *The Journal of biological chemistry 276*, 3254-3261.

(8) Tiwari, P. M., Eroglu, E., Bawage, S. S., Vig, K., Miller, M. E., Pillai, S., Dennis, V. A., and Singh, S. R. (2014) Enhanced intracellular translocation and biodistribution of gold nanoparticles functionalized with a cell-penetrating peptide (VG-21) from vesicular stomatitis virus. *Biomaterials 35*, 9484-9494.

(9) Kristensen, M., Birch, D., and Mørck Nielsen, H. (2016) Applications and Challenges for Use of Cell-Penetrating Peptides as Delivery Vectors for Peptide and Protein Cargos. *International Journal of Molecular Sciences 17*, 185.

(10) Connor, E. E., Mwamuka, J., Gole, A., Murphy, C. J., and Wyatt, M. D. (2005) Gold nanoparticles are taken up by human cells but do not cause acute cytotoxicity. *Small (Weinheim an der Bergstrasse, Germany) 1*, 325-327.

(11) Ghosh, P., Han, G., De, M., Kim, C. K., and Rotello, V. M. (2008) Gold nanoparticles in delivery applications. *Advanced Drug Delivery Reviews 60*, 1307-1315.

(12) Giljohann, D. A., Seferos, D. S., Daniel, W. L., Massich, M. D., Patel, P. C., and Mirkin, C. A. (2010) Gold nanoparticles for biology and medicine. *Angew Chem Int Ed Engl 49*, 3280-3294.

(13) Pissuwan, D., Niidome, T., and Cortie, M. B. (2011) The forthcoming applications of gold nanoparticles in drug and gene delivery systems. *Journal of Controlled Release 149*, 65-71.

(14) Sapsford, K. E., Berti, L., Medintz, I. L., and Begley, T. P. (2007) Fluorescence Spectroscopy: Applications in Chemical Biology, in *Wiley Encyclopedia of Chemical Biology*, John Wiley & Sons, Inc.

(15) Rozenzhak, S. M., Kadakia, M. P., Caserta, T. M., Westbrook, T. R., Stone, M. O., and Naik, R. R. (2005) Cellular internalization and targeting of semiconductor quantum dots. *Chemical Communications*, 2217-2219.

(16) Sosibo, M. N., Keter, K. F., Skepu, A., Tshikhudo, T. R., and Revaprasadu, N. (2015) Facile Attachment of TAT Peptide on Gold Monolayer Protected Clusters: Synthesis and Characterization. *Nanomaterials 5*.

(17) Wagner, S. C., Roskamp, M., Colfen, H., Bottcher, C., Schlecht, S., and Koksch, B. (2009) Switchable electrostatic interactions between gold nanoparticles and coiled coil peptides direct colloid assembly. *Organic & Biomolecular Chemistry 7*, 46-51.

(18) de la Fuente, J. M., and Berry, C. C. (2005) Tat Peptide as an Efficient Molecule To Translocate Gold Nanoparticles into the Cell Nucleus. *Bioconjugate Chemistry 16*, 1176-1180.

(19) Ojea-Jiménez, I., García-Fernández, L., Lorenzo, J., and Puntes, V. F. (2012) Facile Preparation of Cationic Gold Nanoparticle-Bioconjugates for Cell Penetration and Nuclear Targeting. *ACS Nano 6*, 7692-7702.

(20) Slocik, J. M., Stone, M. O., and Naik, R. R. (2005) Synthesis of Gold Nanoparticles Using Multifunctional Peptides. *Small (Weinheim an der Bergstrasse, Germany) 1*, 1048-1052.

(21) Tran, N. T. T., Wang, T.-H., Lin, C.-Y., Tsai, Y.-C., Lai, C.-H., Tai, Y., and Yung, B. Y. M. (2011) Direct Synthesis of Rev Peptide-Conjugated Gold Nanoparticles and Their Application in Cancer Therapeutics. *Bioconjugate Chemistry 22*, 1394-1401.

(22) Yin, H.-Q., Mai, D.-S., Gan, F., and Chen, X.-J. (2014) One-step synthesis of linear and cyclic RGD conjugated gold nanoparticles for tumour targeting and imaging. *RSC Advances 4*, 9078-9085.

(23) Unal Gulsuner, H., Ceylan, H., Guler, M. O., and Tekinay, A. B. (2015) Multi-Domain Short Peptide Molecules for in Situ Synthesis and Biofunctionalization of Gold Nanoparticles for Integrin-Targeted Cell Uptake. *ACS Applied Materials & Interfaces 7*, 10677-10683.

(24) Rai, A., Pinto, S., Velho, T. R., Ferreira, A. F., Moita, C., Trivedi, U., Evangelista, M., Comune, M., Rumbaugh, K. P., Simoes, P. N., Moita, L., and Ferreira, L. (2016) One-step synthesis of high-density peptide-conjugated gold nanoparticles with antimicrobial efficacy in a systemic infection model. *Biomaterials 85*, 99-110.

(25) Yang, H., Fung, S.-Y., and Liu, M. (2011) Programming the Cellular Uptake of Physiologically Stable Peptide–Gold Nanoparticle Hybrids with Single Amino Acids. *Angewandte Chemie International Edition 50*, 9643-9646.

(26) Serizawa, T., Hirai, Y., and Aizawa, M. (2009) Novel Synthetic Route to Peptide-Capped Gold Nanoparticles. *Langmuir 25*, 12229-12234.

(27) Derjaguin, B. V., and Landau, L. (1941) Theory of the Stability of Strongly Charged Lyophobic Sols and of the Adhesion of Strongly Charged Particles in Solutions of Electrolytes. *Acta Phys. Chim. URSS 14*, 633-662.

(28) Ojea-Jiménez, I., and Puntes, V. (2009) Instability of Cationic Gold Nanoparticle Bioconjugates: The Role of Citrate Ions. *Journal of the American Chemical Society 131*, 13320-13327.

(29) Xie, J., Lee, J. Y., Wang, D. I. C., and Ting, Y. P. (2007) Silver Nanoplates: From Biological to Biomimetic Synthesis. *ACS Nano 1*, 429-439.

(30) Xie, J., Zheng, Y., and Ying, J. Y. (2009) Protein-Directed Synthesis of Highly Fluorescent Gold Nanoclusters. *Journal of the American Chemical Society 131*, 888-889.

(31) Ji, X., Song, X., Li, J., Bai, Y., Yang, W., and Peng, X. (2007) Size Control of Gold Nanocrystals in Citrate Reduction: The Third Role of Citrate. *Journal of the American Chemical Society 129*, 13939-13948.

(32) Link, S., and El-Sayed, M. A. (1999) Size and Temperature Dependence of the Plasmon Absorption of Colloidal Gold Nanoparticles. *The Journal of Physical Chemistry B 103*, 4212-4217.

(33) Cui, Y., Wang, Y., Liu, R., Sun, Z., Wei, Y., Zhao, Y., and Gao, X. (2011) Serial Silver Clusters Biomineralized by One Peptide. *ACS Nano 5*, 8684-8689.

(34) Ruzza, P., Calderan, A., Guiotto, A., Osler, A., and Borin, G. (2004) Tat cell-penetrating peptide has the characteristics of a poly(proline) II helix in aqueous solution and in SDS micelles. *Journal of peptide science : an official publication of the European Peptide Society 10*, 423-426.

(35) Hamley, I. W., Dehsorkhi, A., Castelletto, V., Furzeland, S., Atkins, D., Seitsonen, J., and Ruokolainen, J. (2013) Reversible helical unwinding transition of a self-assembling peptide amphiphile. *Soft Matter 9*, 9290-9293.

(36) Karki, I., Wang, H., R Geise, N., Wilson, B., Lewis, J., and Gullion, T. (2015) *Tri-peptides on Gold Nanoparticles: Structural Differences Between Two Reverse Sequences as Determined by Solid-State NMR and DFT Calculations*, Vol. 119.

(37) De Palma, R., Peeters, S., Van Bael, M. J., Van den Rul, H., Bonroy, K., Laureyn, W., Mullens, J., Borghs, G., and Maes, G. (2007) Silane Ligand Exchange to Make Hydrophobic Superparamagnetic Nanoparticles Water-Dispersible. *Chemistry of Materials 19*, 1821-1831.

(38) Li, G., Li, D., Zhang, L., Zhai, J., and Wang, E. (2009) One-step synthesis of folic acid protected gold nanoparticles and their receptor-mediated intracellular uptake. *Chemistry (Weinheim an der Bergstrasse, Germany) 15*, 9868-9873.

(39) Porta, F., Speranza, G., Krpetić, Ž., Dal Santo, V., Francescato, P., and Scarì, G. (2007) Gold nanoparticles capped by peptides. *Materials Science and Engineering: B 140*, 187-194.

(40) Leff, D. V., Brandt, L., and Heath, J. R. (1996) Synthesis and Characterization of Hydrophobic, Organically-Soluble Gold Nanocrystals Functionalized with Primary Amines. *Langmuir 12*, 4723-4730.

(41) Turkevich, J., Stevenson, P. C., and Hillier, J. (1951) A study of the nucleation and growth processes in the synthesis of colloidal gold. *Discussions of the Faraday Society 11*, 55-75.

(42) Zor, T., and Selinger, Z. (1996) Linearization of the Bradford protein assay increases its sensitivity: theoretical and experimental studies. *Analytical biochemistry 236*, 302-308.

(43) Bradford, M. M. (1976) A rapid and sensitive method for the quantitation of microgram quantities of protein utilizing the principle of protein-dye binding. *Analytical biochemistry 72*, 248-254.

(44) Liu, X., Atwater, M., Wang, J., and Huo, Q. (2007) Extinction coefficient of gold nanoparticles with different sizes and different capping ligands. *Colloids and Surfaces B: Biointerfaces 58*, 3-7.

(45) Liu, H., Shen, M., Zhao, J., Guo, R., Cao, X., Zhang, G., and Shi, X. (2012) Tunable synthesis and acetylation of dendrimer-entrapped or dendrimer-stabilized gold-silver alloy nanoparticles. *Colloids and surfaces. B, Biointerfaces 94*, 58-67.

(46) Sanz, V., Conde, J., Hernández, Y., Baptista, P. V., Ibarra, M. R., and de la Fuente, J. M. (2012) Effect of PEG biofunctional spacers and TAT peptide on dsRNA loading on gold nanoparticles. *Journal of Nanoparticle Research 14*, 917.

(47) Shi, Y., Wan, A., Shi, Y., Zhang, Y., and Chen, Y. (2014) Experimental and mathematical studies on the drug release properties of aspirin loaded chitosan nanoparticles. *BioMed research international 2014*, 613619.

(48) Shukla, R., Bansal, V., Chaudhary, M., Basu, A., Bhonde, R. R., and Sastry, M. (2005) Biocompatibility of gold nanoparticles and their endocytotic fate inside the cellular compartment: a microscopic overview. *Langmuir 21*, 10644-10654.

(49) Pandey, S., Oza, G., Mewada, A., Shah, R., Thakur, M., and Sharon, M. (2013) Folic acid mediated synaphic delivery of doxorubicin using biogenic gold nanoparticles anchored to biological linkers. *Journal of Materials Chemistry B 1*, 1361-1370.

(50) Shi, J., Votruba, A. R., Farokhzad, O. C., and Langer, R. (2010) Nanotechnology in Drug Delivery and Tissue Engineering: From Discovery to Applications. *Nano Letters 10*, 3223-3230.